



# IJPPR

INTERNATIONAL JOURNAL OF PHARMACY & PHARMACEUTICAL RESEARCH  
An official Publication of Human Journals

ISSN 2349-7203




Human Journals

**Research Article**


March 2017 Vol.:8, Issue:4

© All rights are reserved by K. Mohana Raju et al.

## Development of Magnetic Nano-Particles Embedded in Hydrogels Based on Sodium Alginate and Gelatin for Biomedical Application



**IJPPR**  
INTERNATIONAL JOURNAL OF PHARMACY & PHARMACEUTICAL RESEARCH  
An official Publication of Human Journals



ISSN 2349-7203

**Bandla Manjula<sup>1</sup>, S.Veerapratap<sup>1</sup>, Rotimi sadiku<sup>2</sup>, K. Mohana Raju\***

<sup>1</sup>*Department of Polymer Science & Technology, Sri Krishnadevaraya University, Anantapur-515 003, A.P. India*

<sup>2</sup>*Tshwane University of Technology, Dept. of Polymer Technology, South Africa.*

**Submission:** 12 March 2017  
**Accepted:** 15 March 2017  
**Published:** 25 March 2017



HUMAN JOURNALS

[www.ijppr.humanjournals.com](http://www.ijppr.humanjournals.com)

**Keywords:** HGMNCs, Sodium Alginate, Gelatin, drug release kinetics.

### ABSTRACT

Most pointedly, magnetic nanoparticles have been widely used in drug delivery and hyperthermia treatment for cancer. However, recent applications of magnetic nanoparticles demonstrate their promise towards decreasing implant infection and increasing tissue progress. To build the most actual magnetic nanoparticle systems for various biomedical applications, particle characteristics including size, surface chemistry, magnetic properties and toxicity have to be fully investigated. The present study deals with the preparation of the loading efficiency of 5-Fu in hydrogels varies by the types of hydrogels. Hydrogel-magnetic nanocomposites (HGMNCs) prepared by employing polysaccharide and magnetic nanoparticles (iron oxide ( $Fe_3O_4$ )). Poly(acrylamide, sodium alginate, gelatin P(AM- SA-GT) hydrogels were synthesized by employing free radical polymerization using ammonium persulfate/*N,N,N',N'*tetramethylethylenediamine (APS/TMEDA) as redox-initiating pair, *N,N*-methylene bisacrylamide (MBA) as a cross-linker following the usual procedure. The loading efficiency of 5-Fu in hydrogels was formulated and characterized by DSC, XRD, FTIR, TEM, VSM & SEM techniques. Further, the drug load magnetic nanoparticles have utilized for drug release studies in terms of drug content, loading efficiency, particle size and *in-vitro* drug release kinetics.

## 1. INTRODUCTION

The study of Magnetic nanoparticles (MNPs) has been the subject of intense research for the last few years because of the potential applications of magnetic nanoparticles as electronic, photonic, magnetic and biomedical materials. Hydrogel-magnetic nanocomposites (HGMNCs) prepared by employing polysaccharide and magnetic nanoparticles (iron oxide ( $\text{Fe}_3\text{O}_4$ ) or maghemite ( $\gamma\text{-Fe}_2\text{O}_3$ )) have been shown, sensitivity to an external stimulus i.e., to an applied magnetic field [1, 2]. Many researchers have studied such hydrogels aiming for controlled release of drugs for targeting cancer cells, separation of biomolecular, immobilization of enzymes and hyperthermia applications.

Sodium alginate and gelatin are two different another components that are frequently used in the preparation of polymeric inorganic composites. Sodium alginate is a complex polysaccharide occurring in the cell walls of the brown algae is a natural Polymer. Because of its unique gelling properties; sodium alginate is an important material for the preparation of hydrogels. As a biomaterial, gelatine a pale yellow water soluble protein also has several advantages. It is a natural polymer having no antigenicity, with complete resorbable in vivo capacity. The physicochemical properties of this material can be suitably modulated. Similarly, due to the presence of large number of functional side groups, sodium alginate readily undergoes chemical cross-linking. This property is very important in the preparation of biomaterials for being used as a drug delivery systems or wound dressing materials. Due to the importance of the above two materials and the magnetic nanocomposites, the present work has been carried out. Hydrogels embedded magnetic nanoparticles have been employed as magnetically modulated drug delivery systems with feasibility of delivering drug at controlled rates. Such drug delivery systems involve the incorporation of large amount of magnetic beads in polymer matrices/hydrogels, and the release profile of the drug was demonstrated to be dependent on magnetic field characteristics (such as external field strength and field amplitude) as well as polymer/hydrogel properties. Hydrogels were developed in the last couple of decades for various biomedical applications because of their inherent unique properties.

Hydrogels due to their water retention, network porosity, elasticity properties enable them for vital applications such as adsorbents in various fields such as scaffolds [3], tissue engineering [4], bioseparation [5], drug delivery [6], and three-dimensional composites [7]. Because of their porous nature hydrogels can offer suitable environment for the development of various

nanoparticles with enhanced stability. Therefore a number of hydrogel magnetic nanocomposites were evaluated for superior biomedical applications [8, 9]. Design of hydrogel magnetic nanoparticle composite materials (ferrogels or magnetic hydrogel) would offer combined magnetic properties in addition to conventional hydrogel characteristics [10]. Variation of cross-linking density, chemical entity and synthetic approach decides the integration of the nanoparticles within the polymer hydrogels matrix that can promote controlled, triggered and hyperthermia applications.

Incorporation of magnetic nanoparticles into hydrogel networks results in hydrogel magnetic nanocomposites, i.e., ferrogels in which the magnetic nanoparticles are stabilized by cross-linked gel networks. This can result in superior interaction between the magnetic nanoparticles and the gel networks thereby improving their mechanical properties. If these ferrogels are constructed by magnetic nanoparticles of typical size of  $< 20$  nm they impart superparamagnetic properties [11]. Hydrogels developed synthesized by employing natural polymers and magnetic materials such as iron oxide ( $\text{Fe}_3\text{O}_4$ ) or maghemite ( $\gamma\text{-Fe}_2\text{O}_3$ ) have been widely used in the development of ferrogel which finds many applications due to their proven biocompatibility, quick response and sensitivity to an external stimulus such as applied magnetic field [12, 13].



From the above discussion, it can be inferred that magnetic nanoparticles embedded in natural polymers or modified natural polymers find many important applications. Keeping this in view the present work involves the development of ferrogels by incorporating magnetic nanoparticles in the hydrogels developed by using two important natural polymers such as sodium alginate and gelatin in the presence of acrylamide. The developed ferrogels are used for drug delivery application using 5-Fluorouracil (5-Fu) an anticancer drug [14].

## 2. EXPERIMENTAL

### 2.1 Materials

Acrylamide (AM), ammonium persulfate (APS), and 5-Fluorouracil (5-Fu) were purchased from Aldrich Chemical Company Inc. *N,N*-methylene bisacrylamide (MBA), *N,N,N',N'*-tetramethylethylenediamine (TMEDA), (Milwaukee, WI, USA), sodium alginate (SA), gelatin (MW 200000) (GT), iron (II) chloride tetrahydrate (99+%) ( $\text{FeCl}_2 \cdot 4\text{H}_2\text{O}$ ) and iron (III) chloride hexahydrate (99+%) ( $\text{FeCl}_3 \cdot 6\text{H}_2\text{O}$ ) were purchased from Merck (Mumbai, India). Ammonium hydroxide (28% ammonia in water) (99.99%) was purchased from S.D. Fine

(Mumbai, India). All the chemicals were used without further purification. Double-distilled water was used for the preparation of all solutions in this study.

## 2.2 Preparation of Gels

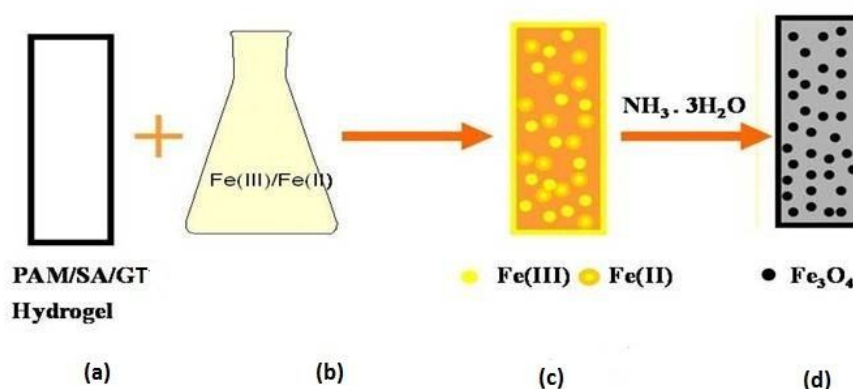
Poly(acrylamide, sodium alginate, gelatin P(AM- SA-GT) hydrogels were synthesized by employing free radical polymerization using ammonium persulfate/*N, N, N<sup>l</sup>, N<sup>l</sup>*-tetramethylethylenediamine (APS/TMEDA) as redox-initiating pair, *N, N*-methylene bisacrylamide (MBA) as a cross-linker following the usual procedure. In detail, PAM-SA-GT hydrogels were prepared by first mixing AM (1 g) with different amounts of Sodium Alginate (SA) (0.1, 0.2, 0.3 g) and Gelatin (GT) (0.1, 0.2, 0.3 g) in 5 mL water. and polymerizing them using ammonia persulfate (APS) and *N,N,N<sup>l</sup>,N<sup>l</sup>*-tetramethyl ethylenediamine (TMEDA) as initiating pair and methylene bisacrylamide (MBA) as were removed washed with distilled water and allowed them to dry in an oven (GUNA, Chennai, India) at 60°C.

**Table: 1. Preparation of Sodium Alginate and Gelatin hydrogels feed composition**

Hydrogels code	AM (gm)	SA (gm)	GT (gm)	APS ( Mmx10 <sup>-3</sup> )	MBA ( Mmx10 <sup>-5</sup> )	TEMEDA ( Mmx10 <sup>-3</sup> )
PAM-SA1-GT	1.0	0.10	0.5	2.197	4.86	1.721
PAM-SA2-GT	1.0	0.20	0.5	2.197	4.86	1.721
PAM-SA3-GT	1.0	0.30	0.5	2.197	4.86	1.721
PAM-SA-GT1	1.0	0.5	0.1	2.197	4.86	1.721
PAM-SA-GT2	1.0	0.5	0.2	2.197	4.86	1.721
PAM-SA-GT3	1.0	0.5	0.3	2.197	4.86	1.721
PAM-SA-GT	1.0	0.5	0.5	2.197	4.86	1.721

### 2.3 Preparation of PAM-SA-GT hydrogels magnetite nanocomposites (PAM-SA-GT-Fe<sub>3</sub>O<sub>4</sub>)

The hydrogel magnetic nanocomposites were prepared by placing PAM-SA-GT dry hydrogel samples (as presented in table 1) individually in 50 mL of double distilled water and allowed them to swell completely over a period of 24 hours. Each individual swollen hydrogel was transferred separately to another beaker containing 200 mL of water consisting of 2.1 g of iron (II) chloride tetrahydrate and 5.8 g of iron (III) chloride hexahydrate and allowed it for 24 hrs to entrap the iron salts throughout the hydrogel networks [15]. Then the hydrogel loaded with iron (II) and iron (III) ions was removed from the iron salt solutions, washed with double distilled water and placed in a beaker consisting 50 mL of 0.5 M ammonium hydroxide (28% NH<sub>3</sub> in water) solution and left overnight. The resultant brown or black color hydrogel magnetic nanocomposite was removed, washed with double distilled water, and allowed to dry in an oven (GUNA, Chennai, India) at 60°C. The schematic diagram of formation of hydrogel magnetic nanocomposite is shown below (Scheme-1).



**Scheme 1: Schematic representation of the synthesis of magnetic hydrogel a) PAM-SA-GT Swollen hydrogel b) ferrous & ferric solution, c) PAM-SA-GT-iron salts loaded hydrogel d) PAM-SA-GT-Fe<sub>3</sub>O<sub>4</sub>**

### 3. SWELLING STUDIES

The dried PAM-SA-GT hydrogels and PAM-SA-GT hydrogel nanocomposites (~ 50 mg) were equilibrated in distilled water at 30°C for 3 days. The equilibrium swelling capacity or swelling ratio (*Q*) of PAM-SA-GT hydrogel and PAM-SA-GT3 hydrogels nanocomposites was calculated following the equation:

$$Q = W_e/W_d, \text{-----} (1)$$

Where  $W_e$  is the weight of water in the swollen gel at equilibrium and  $W_d$  is the dry weight of the dried gel.

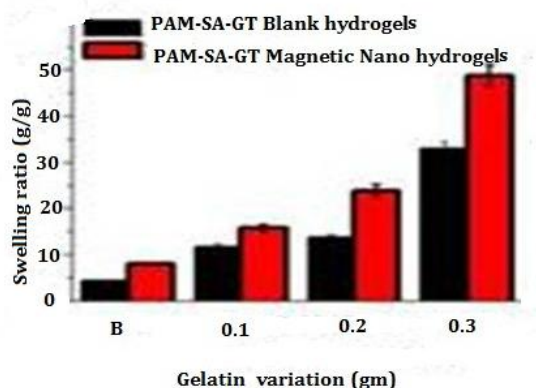


**Fig: 1. Swelling capacity of various hydrogels synthesized with different composition of PAM-SA-GT hydrogel and PAM-SA-GT-Nano hydrogel.**

#### 4. CHARACTERIZATION

##### 4.1. UV-Vis spectrophotometer



UV-Vis absorption spectra of the hydrogels drug delivery were recorded on a Elico SL 160A Model UV-Vis spectrophotometer at  $\lambda_{max}$  266.5 nm.

**4.2. FTIR Spectroscopy:** FTIR Spectroscopy was performed for, PAM-SA-GT & PAM-SA-GT-iron salts loaded & PAM-SA-GT- $Fe_3O_4$  samples using Termo Nicolet Nexus 670 Spectrophotometer (Washington, USA) by KBr pellet method.

**4.3. X-Ray Diffraction:** X-ray diffraction studies of PAM-SA-GT3 hydrogel, PAM-SA-GT3 and PAM-SA-GT3- $Fe_3O_4$  samples were carried out using a Rigaku diffractometer, (Rikagu, Tokyo, Japan) employing rotating anode mode Ru-H3R (Cu radiation,  $k = 0.1546$  nm) running at 40 kV and 40 mA.

**4.4. Scanning Electron Microscopy (SEM):** The surface morphology of PAM-SA-GT3 blank hydrogel, PAM-SA-GT3 iron salts loaded hydrogel, and PAM-SA-GT3- $Fe_3O_4$  samples were studied using a JEOL JSM 840A (Tokyo, Japan) scanning electron microscope (SEM) at an accelerating voltage of 15 kV. All the samples were dried in vacuum at room temperature and coated with gold before scanning.

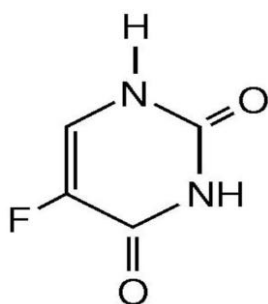
**4.5. Transmission Electron Microscopy (TEM):** The size of the magnetic nanoparticles in gel network was determined using a Technai F12 TEM (Philips Electron Optics, Holland). TEM samples were prepared by dropping 2–3 drops of aqueous solutions of magnetic nanoparticles on a 200 mesh formvar-coated copper TEM grid (grid size: 97  $\mu\text{m}$ ) (Ted Pella, Inc., Redding, CA, USA) and then removing excess solution using a piece of fine filter paper and the samples were allowed to dry in air overnight prior to image the particles. The particle size of magnetic nanoparticles in TEM images was measured using NIH Image software (<http://rsbweb.nih.gov/ij/>).

**4.6. Magnetization studies using VSM:** The magnetization and hysteresis loop were measured at room temperature using a Vibrating Sample Magnetometer (Model 7300 VSM system, Lake Shore Cryotronic, Inc. Westerville OH, USA)

#### 4.7. Drug loading and releasing

5-Fluorouracil (5-Fu) is a drug used in cancer chemotherapy. It is closely related to the. 5-Fu is commonly used in the treatment of a wide range of cancers, including hematological malignancies, many types of carcinoma, and soft tissue sarcomas. Therefore, this compound is chosen to load into the hydrogels for drug delivery applications. The 5-Fu drug was loaded in the hydrogel samples by immersing the hydrogel in the drug solution. Experimentally, 50 mg of hydrogel sample was taken and immersed in 20 mL of drug solution (5 mg/ 20 mL distilled water). The amount of drug included in the hydrogel sample was determined by UV-Vis spectroscopy. To determine the maximum absorbance of 5-Fu, the UV-Vis spectra for pure drug solution was taken and the maximum absorbance is found at  $\lambda_{\text{max}}$  270.5 nm. The % of drug loading was calculated using the following equation.

$$\% \text{ Encapsulation efficiency} = [\% \text{ actual loading} / \% \text{ theoretical loading}] \times 100 \text{ -----(3)}$$



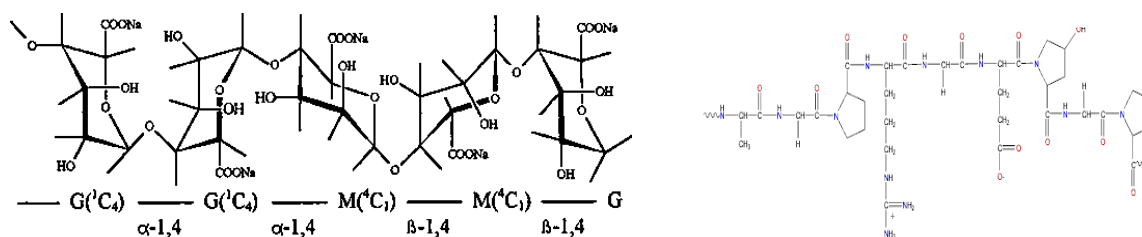
Structure of 5-fluorouracil

#### 4.8. Release of 5-Floro Urasil

The in vitro release studies of the 5-Fu drug were carried out by placing the dried and 5-Fu loaded hydrogel indefinite volume (50 ml) of releasing medium (7.4 pH phosphate buffer (PBS) and the dissolution medium was placed in a rotary shaker (Remi Instruments Limited, Model No CIS-24BL, Vasai, India) at 100 rpm at 37°C. The amount of drug release was measured spectrophotometrically in pH 7.4 buffer solution. The absorptions of the solutions of 5-Fu drug were measured at  $\lambda_{max}$  270.5 nm. The results are shown in Fig.9. in the results & discussion.

### 5. RESULTS AND DISCUSSION

Acrylamide based polymers interact with many other polymers or molecules due to the existence of amide groups (CONH<sub>2</sub>) in the main chains. The acrylamide hydrogels can easily bind to the iron (II) and iron (III) cations in aqueous mixed solutions of iron (II) chloride tetrahydrate and iron (III) chloride hexahydrate via electrostatic interactions. Similarly, Sodium alginate (SA) and gelatin (GT), the two other hydrophilic and biodegradable components of the hydrogel have been found to exert an appreciable influence on the water absorption characteristics of the hydrogel. Therefore the combination of these three is used in the synthesis of hydrogel network template for *in situ* deposition of magnetic iron oxide particles by utilizing the reduction route induced by ammonia solution. The concept of magnetic nanoparticles synthesis in PAM hydrogel networks and stabilization of Fe<sub>3</sub>O<sub>4</sub> nanoparticles by sodium alginate and gelatin is schematically in Scheme-1 in experimental section 3.2.3.



**Structure of Sodium Alginate (C<sub>6</sub>H<sub>7</sub>NaO<sub>6</sub>)<sub>n</sub>**

Gelatin is a heterogeneous mixture of single or multi-stranded polypeptides, each with extended left-handed proline helix conformations and containing between 50 - 1000 amino acids. The triple helix of type I collagen extracted from skin and bones, as a source for gelatin, is composed of two  $\alpha$ 1(I) and one  $\alpha$ 2(I) chains, each with molecular mass ~95 kD,



width  $\sim 1.5$  nm and length  $\sim 0.3$   $\mu\text{m}$ . Gelatin consists of mixtures of these strands together with their oligomers and breakdown (and other) polypeptides. Solutions undergo coil-helix transition followed by aggregation of the helices by the formation of collagen-like right-handed triple-helical proline/hydroxyproline rich junction zones.

Gelatin is primarily used as a gelling agent forming transparent elastic thermoreversible gels on cooling below about  $35^\circ\text{C}$ , which dissolve at low temperature to give 'melt in the mouth' products with useful flavour-release. In addition, the amphiphilic nature of the molecules endows them with useful emulsification (for example, whipped cream) and foam-stabilizing properties (for example, mallow foam). On dehydration, irreversible conformational changes take place [397] that may be used in the formation of surface films. Such films are strongest when they contain greater triple-helix content. Although gelatin is by far the major hydrocolloid used for gelling and Gelatin is nutritionally lacking as a protein being deficient in isoleucine, methionine, threonine and tryptophan.

### 5.1 Swelling Studies:

In the present study, the swelling capacity of various PAM-SA-GT hydrogels prepared by varying SA (0.10,0.20,0.30 g) and GT (0.1,0.2,0.3 g) separately was studied. By increasing the two natural polymers separately by keeping one constant in the hydrogel network has increased the swelling capacity of the hydrogels. This is due to the presence of more hydrophilic groups such as  $-\text{NH}_2$ ,  $-\text{COOH}$  and amide linkages in the hydrogel networks, which assist in improving the swelling capacity. The increase in the swelling capacity was still more in the case of magnetic nanocomposites. This pattern of swelling is reasonable for magnetic nanocomposites because once the magnetic nanoparticles are formed inside the gel networks, the overall porosity of the system increases allowing more number of water molecules inside the gel [16]. One more reason for this behavior is that the formed nanoparticles have different sizes with different surface charges in the gel networks causing absolute expansion of the networks.

## 6. CHARACTERIZATION

### 6.1 FTIR spectroscopy

The formation of magnetic nanoparticles in the hydrogel networks was confirmed by FTIR spectroscopy and X-ray diffraction studies. The FTIR spectra of PAM-SA-GT Blank hydrogel PAM-SA-GT3 iron salt loaded hydrogel and PAM-SA-GT3 hydrogel magnetic

nanocomposites are presented in Figure 2. In all the samples, common peaks related to  $\text{NH}_2$ ,  $\text{COOH}$  and  $\text{CO-NH}$  groups were observed at  $3432\text{ cm}^{-1}$ ,  $3158\text{ cm}^{-1}$ ,  $1665\text{ cm}^{-1}$  and  $1462\text{ cm}^{-1}$  due to  $\text{NH}_2$  groups, amide groups, and carbonyl groups of different units present in the gel structure respectively. An addition a peak at  $601\text{ cm}^{-1}$  was observed in the case of magnetic nanocomposites (C) (due to the presence of iron oxide nanoparticles). This is a common stretching peak observed for Fe-O vibrations of  $\text{Fe}_3\text{O}_4$  nanoparticles. This confirms the presence of iron oxide nanoparticles in the hydrogel networks.

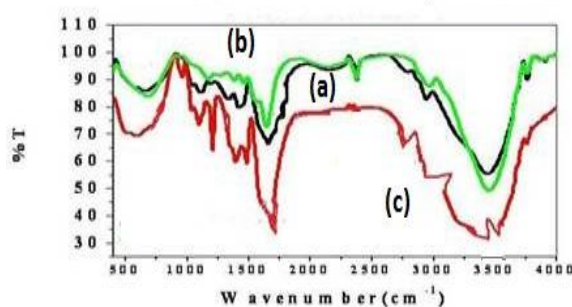


**Fig 2. IR spectra of a) PAM-SA-GT3 Blank, b) PAM-SA-GT3-Iro salta loaded c) PAM-SA-GT3-Fe<sub>3</sub>O<sub>4</sub>**

## 6.2 X-ray Diffraction (XRD):



To study the crystallographic nature of Iron oxide nanoparticles and the nanocomposite the XRD analysis was performed and the corresponding XRDs are shown in Figure 3. PAM-SA-GT and PAM-iron salts loaded hydrogels have not exhibited any sharp peaks in XRD. A broad peak at  $2\theta$  is due to the polymer network. In the case of hydrogel magnetic nanocomposite, sharp peaks are observed at  $2\theta = 29.9^\circ$ ,  $35.03^\circ$ ,  $42.6^\circ$ ,  $53.2^\circ$ ,  $56.8^\circ$ , and  $62.3^\circ$ . The well defined X-ray diffraction patterns indicate the formation of highly crystalline iron oxide nanoparticles. The results also indicate that the prepared nanoparticles are pure magnetite with an inverse cubic spinal structure, which is identical to the standard XRD patterns of  $\text{Fe}_3\text{O}_4$ .

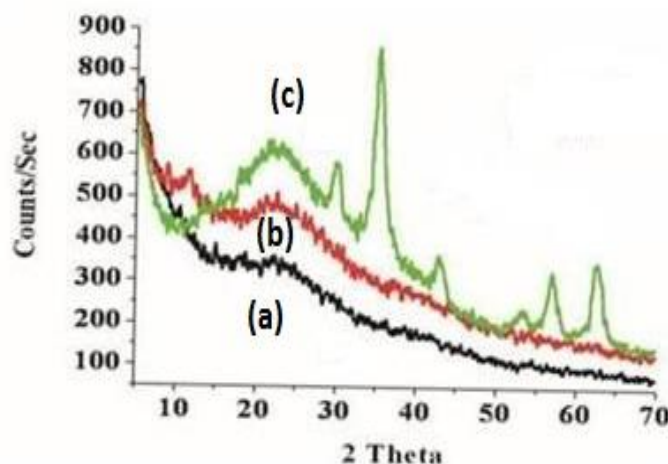


**Fig: 3 XRD patterns of a) PAM-SA-GT Blank hydrogel b) PAM-SA-GT3 –Iron salts loaded hydrogel c) PAM-SA-GT3-Fe<sub>3</sub>O<sub>4</sub>**

### 6.3 Morphology Studies: SEM&TEM Analysis:

**6.4 Scanning electron microscopy(SEM)** The surface morphology of PAM-SA-GT3 blank hydrogel, PAM-SA-GT3 iron salt loaded hydrogel and PAM-SA-GT3-Fe<sub>3</sub>O<sub>4</sub> are shown in Figure 4a clear and uniform surface morphology was observed for the PAM-SA-GT3 hydrogel (Figure 4A), whereas iron salt loaded PAM-SA-GT3 hydrogel has shown a randomly aggregated structure throughout the gel network (Figure 4b). However, there is a pinpoint variation in the case of PAM-SA-GT-Fe<sub>3</sub>O<sub>4</sub> Figure 4C. This clearly illustrates the formation of well defined magnetic nanostructures throughout the hydrogel networks. This indicates the formation of magnetic nanoparticles within the PAM-SA-GT3 chains rather than just entrapment in the gel networks. Most of the entrapped particles might have extracted during the purification step of magnetic nanocomposite synthesis. The use of sodium alginate and gelatin in the networks is to stabilize the formed magnetic nanoparticles and keep them intact within the hydrogel networks.

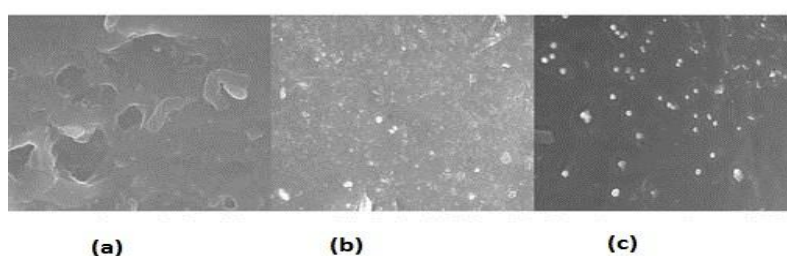


**Fig:4 SEM images of a) PAM-SA-GT Blank b) PAM-SA-GT3-Iro salts loaded c) PAM-SA-GT<sub>3</sub>-Fe<sub>3</sub>O<sub>4</sub>**

### 6.5 Transmission electron microscopy (TEM):

Transmission electron microscopy provides very useful information about the size of particle, polydispersity profile, and location of the magnetite nanoparticles inside and outside of the hydrogel. Numbers of particles have increased with increase of GT content. These images indicate that the formation of magnetic nanocomposites is more with increase of GT within the hydrogel network. These compositions permit the establishment of inter and intramolecular attractions between the hydrogel networks due to less free space within the hydrogel networks. This ultimately helps not only in controlling the size of the nanoparticles but also provides better stabilization of them for longer periods. The TEM image is presented in fig.5

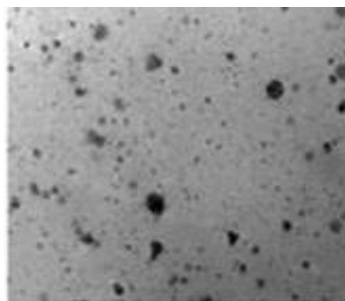


**Fig: 5 The TEM images shows the size of magnetic nanoparticle is of 15 and 16 nm for PAM-SA-GT3-Fe<sub>3</sub>O<sub>4</sub>**

### 6.6 Magnetic Properties:

#### 6.7 Vibrating Sample Magnetometer (VSM)

The characteristic of an ideal superparamagnetic material with a size of less than 20 nm is to have zero coercivity and zero remanence [17]. The magnetization curve was determined from Vibrating Sample Magnetometer and presented in fig.6

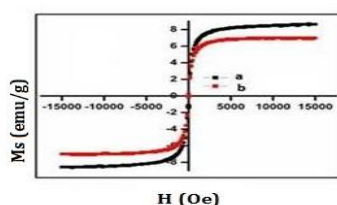


**Fig 6: Magnetization curve of PAM-SA-GT3 Fe<sub>3</sub>O<sub>4</sub>.**

The variation in the magnetic moment of the hydrogel magnetic nanocomposites was investigated as a function of varying the magnetic field in the range of -15000 to 15000 Oe. The saturation magnetization ( $M_s$ ) for the Iron salts loaded PAM-SA- GT3 - $Fe_2O_4$  was found to be 6.5 emu/g. In the case of PAM-SA- GT3 - $Fe_3O_4$  the  $M_s$  value was found to be 8.6 emu/g. From these calculations, it can be assumed that the present composites containing single domain of magnetic nanoparticles within the hydrogel networks exhibit a unique phenomenon of superparamagnetism.

### 6.8 Drug Loading and releasing studies

The loading efficiency of 5-Fu in hydrogels varies by the types of hydrogels. The order of efficiency as noticed was PAM-SA-GT3- $Fe_3O_4$  > PAM-SA-GT3 iron salt loaded hydrogel > PAM-SA-GT3-hydrogel. The higher loading in magnetic nanocomposites is due to the presence of more amount of free space between the hydrogel networks because of nanoparticles formation as well as the 5-Fu molecules can also bind onto the surface of the nanoparticles. It also depends on the amount of GT present in the hydrogel system: In detail, increase of GT units (-CO-NH-groups) holds more number of drug molecules. Overall, the drug loading efficiency depends on the swelling behavior of IPN hydrogels which provides the path for the drug to enter inside the hydrogel networks.

Further, the loading efficiency is more in the presently developed formulations when compared to in conventional hydrogel formulations, i.e., ~16 mg in 100mg of hydrogel. It is also proved that the drug clusters are present on the surface of the hydrogels. The SEM image represents that due to drug addition to PAM-SA-GT3- $Fe_3O_4$  formulation, the entire cross-links were buried with the drug and the excess bound drug can be seen as clumps on the surface of the gel (Figure 7b).

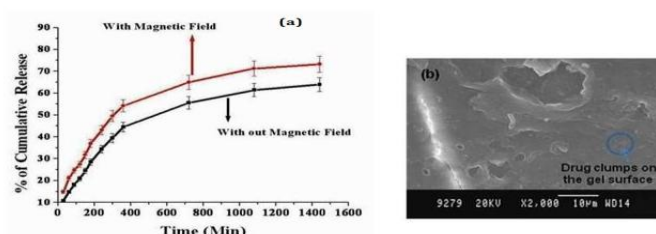


**Fig: 7 a) 5-Fluorouracil release of a) PAM-SA-GT3- $Fe_3O_4$  b) SEM image of drug clump.**

It is well known that the delivery of drugs from the hydrogels system can be controlled by external stimuli (in this case by using external magnetic field). The 5-Fu release from the

magnetic nanocomposite was found to be in a sustained manner (Figure 7 a). Low molecule amounts are entrapped in the hydrogels. Therefore, these gels show a sustained drug release profiles. But, by employing an external applied magnetic field such as a magnetic has improved the delivery of 5-Fu from magnetic nanocomposite into the medium. The experimental results have shown increase at all stages of drug release i.e., at all time points. An improved release is caused by the alignment of magnetic nanoparticles by the external magnetic field which in turn expands the hydrogels networks that allow more number of 5-Fu molecules to release into the medium.

## 7. CONCLUSIONS

Poly (Acrylamide –Sodium Alginate-Gelatin) (PAM-SA-GT) hydrogels as well as PAM-SA-GT hydrogel magnetic nanocomposites (PAM-SA-GT-Fe<sub>3</sub>O<sub>4</sub>) were prepared by using MBA as a cross-linker. The formation of magnetic nanoparticles within the hydrogel network structure was confirmed by using SEM and TEM. The prepared gels were characterized by FTIR spectroscopy and, X-ray diffraction, studies. Their inherent swelling properties were also investigated in detail. The magnetic properties of the developed hydrogel magnetic nanocomposite were studied in detail. The increase of gelatin amount increases the formation of more amount of Fe<sub>3</sub>O<sub>4</sub> nanoparticles as evidenced by SEM and TEM analysis. The drug releasing profiles of the magnetic hydrogels samples were also studied under magnetic field. The prepared magnetic polymer matrices have exhibited both superparamagnetic and biocompatible properties and are useful as potential candidates for biomedical applications. Therefore these studies are highly useful in biomedical applications.

This investigation is an important contribution in the field of site drug delivery systems by using external magnetic field for hyperthermia applications.

The work presented in this chapter is communicated for Publication of Journal of Polymers and Environment.

## 8. REFERENCES

1. S. Rana, A. Gallo, R.S. Srivastava, (2007) R. D. K. Misra, *Acta Biomater*, 3, 233.
2. J. Yang, S.B. Park, H.G.Yoon, Y.M.Huh, S.Haam, (2006) *Int J Pharm*. 324,185.
3. Y. Zhang, N. Kohler, M. Zhang, (2002) *Biomaterials*. 23, 1553.
4. C. H. Cunningham, T. Arai, P.C. Yang, M. V. Mcconnell, J. M. Pauly, S. M. Conolly( 2005) *Magnetic Resonance in Medicine*. 53 999.
5. S.A. Anderson, R.K. Rader, W.F. Westlin, C. Null, D. Jackson, G.M. Lanza, (2000) S. A. *Magnetic Resonance in Medicine*.44, 3433.
6. B. Polyak, G. Friedman, (2009) Expert opinion on drug delivery. 6, 53.
7. G. Reiss, A. Huetten, (2005) *Nat Mater* 4, 725.
8. F. Y. Chang, C. H. Su, Y.S. Yang, C.S. Yeh, C. Y. Tsai, C. L. Wu, M.T. Wu, D.B. Shieh, (2005) *Biomaterials*. 26,729.
9. P. Tartaj, C. J. Serna, (2003) *Journal of the American Chemical Society*.125, 51, 15754.
10. W.T.K. Stevenson, M.V.J. Sefton, (1988) *J. Appl Polym Sci*. 36, 1541.
11. W. E. Roorda, H.E. Bodde, A. G. De Boer, H.E. Junginger, (1986) *Pharmacol Weekblad Sci Ed* 8, 165.
12. S. H. Huang, M. H. Liao, ( 2003) D. H. *Chen, Biotechnol Prog* .19,3,1095.
13. W. J. Freeman, Ndn, (2005) *J Integr Neurosci* .4,4, 407.
14. Zachary N Russ, (2008) *J Biolo Engineering*, 2, 7.
15. K. Samba Sivudu, K.Y. Rhee, (2009) *Colloids and Surfaces A: Physicochem. Eng. Aspects* 349, 29.
16. N.T. K. Thanh, I. Robinson, L. D. Tung, (2007) *Dekker Encyclopedia of Nanoscience and Nanotechnology*.
17. H.G.Shinouda, A.A.Hanna, (1977) *J. Appl. Polym. Sci* 21, 1479.

